PARALLEL ITERATIVE SOLUTION SCHEMES FOR THE ANALYSIS OF AIR FOIL BEARINGS

N. Wang * **S.-H. Chang**

Department of Mechanical Engineering
Chang Gung University
Tao-Yuan, Taiwan 33302, R.O.C.

ABSTRACT

In an air foil bearing analysis the model is usually solved iteratively due in part to the nonlinearity of the modeling Reynolds equation and the compliance of the bearing surface. The solution procedure requires a multiple-level-deep nested iteration, which involves extended solution time and convergence difficulty. In this study, a simple air foil bearing model is used and the compressible-fluid Reynolds equation for modeling gas lubrication is linearized by Newton's method. The discretized equation is solved by one of the two parallel iterative methods, red-black or strip partition successive-over-relaxation (SOR) method. The parallel programming is conducted using OpenMP programming in an eight-core workstation. Then, a numerical damping scheme for the film-profile convergence is presented. Finally, a root-finding process is conducted to iteratively attain the eccentricity of the bearing for a given load. It is found that the numerical damping step is crucial, which allows the use of a larger relaxation factor to have a fast rate of convergence. Both the parallel SOR methods are easy to implement and the red-black SOR method exhibits better efficiency in the studied cases. This study presents a parallel computing scheme for analyzing air foil bearing of bump-type by today's shared-memory multicore platforms.

Keywords: Air foil bearing, Reynolds equation, Relaxation method, Parallel computing.

1. INTRODUCTION

The importance and potential applications of gas or air foil bearing is noted and investigated by many studies for more than two decades. The copious outcomes of the foil bearing studies are based on experimental works [1-3], numerical analysis [4-6], or both [7-9]; Foil gas bearings are self-acting hydrodynamic bearings made from sheet metal foils comprised of at least two layers. The innermost "top foil" layer traps a gas pressure film that supports a load while a layer or layers underneath provide an elastic foundation [1]. An important mechanism influencing foil bearing operation is that the hydrodynamic gas film pressure causes a corresponding elastic deflection of the foil elements [10]. As a result, the foil bearing has evolved into many forms [1]. Also, the working temperature of the machinery equipped with foil bearings is usually high, which raises the temperature of the components and the lubricant (air) of the foil bearings. The elevated temperature demands an efficient thermal management [11] for effective operation. The result of high temperature affects the properties of the foils, the top foil supporting material, and air viscosity. An extended review of thermal effect on air foil bearings can be found in some recent studies [8,9].

In an air foil bearing analysis [12-19] the numerical model needs to be solved iteratively due largely to the nonlinearity of the Reynolds equation and the compliance of the bearing surface. Since the compressible-fluid Reynolds equation for air foil bearing modeling is a nonlinear partial differential equation (PDE) of second-order, the equation is to be solved in a two-level-deep iteration using Newton's method [20]. Due to the compliance of the foil bearing surface the film pressure is an implicit function of the foil (film) profile. The change of the foil profile affects the film pressure, which in turn influences the foil profile. Therefore, for a given eccentricity (shaft position) the bearing model needs to be solved iteratively until both the pressure and profile of the film are converged. Furthermore, for a given bearing load the final compliant foil profile is to be obtained by an iterative root-finding process, in which the eccentricity is to be sought to produce a load equals the applied load. Therefore, a problem of multiple-level-deep nested iteration is constructed. The solver for the linearized PDE, which is required in the inner-most level, is to be applied many times in an air foil bearing analysis.

Salehi and Heshmat [14] applied the successive-over-relaxation (SOR) method to solve the film pressure and the thickness of the bearing. It is noted the number of iterations varied in a wide range in the analysis. Nevertheless, only the cases with relatively

* Corresponding author (nenzi@mail.cgu.edu.tw)

DOI : 10.1017/jmech.2012.50
Copyright © 2012 The Society of Theoretical and Applied Mechanics, R.O.C.
https://doi.org/10.1017/jmech.2012.50 Published online by Cambridge University Press

small eccentricity ratios (0.1 to 0.8) were studied. Note that the eccentricity ratio of an air foil bearing may well exceed unity in many instances (due to the deformation of the foil surface in high pressure). Lee *et al*. [15] studied the influence of the slip flow on steady-state load capacity, stiffness and damping coefficients of gas foil bearings. The successive-under-relaxation (SUR) method was used, in which the relaxation factor is less than one. Peng and Khonsari [16,17] applied the direct fixed-point (DFI) iterative method to transform the Reynolds equation to a form can be solved iteratively. And the Gauss-Seidel (GS) method was applied to solve the discretized equation. The GS method is a special case of the SOR method, in which the relaxation factor is one. They indicated that the simulations with large bearing numbers and high eccentricity ratios require extended solution time. Park *et al*. [18] applied finite difference method to discretize Reynolds equation and applied the SUR method to solve static film pressure and thickness of an air foil thrust bearing. Iordanoff *et al*. [19] considered the effect of dry frictions on foil bearings and applied the GS method as the solver.

None of the aforementioned studies [14-19] were carried out by using parallel computing in the analysis. The numerical convergence problem may occur in the cases of high eccentricity ratio if the solution methods are not properly chosen. This may be the reason the SUR method is applied in some studies. The drawback of the SUR method is extended solution time requirement. It is also well recognized that the SOR method can be very efficient than the GS method when an optimum relaxation factor is used [21,22].

Wang *et al*. [23] compares several approaches for solving compressible-fluid Reynolds equation in modeling air bearings. The approaches, including the linearization method and iterative solver, are compared based on the computation conducted in serial. They concluded that Newton's method shows its effectiveness over the simple DFI method when the same iterative solver is used. They found that the multigrid method is an order faster than the preconditioned conjugate gradient method and the optimum SOR method (the one with an optimum relaxation factor). However, they also indicate that the SOR method can easily deal with discontinued film profile, such as in aerostatic bearing with recesses as boundary. The SOR method is also known for its straightforward implementation and easy to carry out in parallel computing.

To reduce the solution time in modeling fluid film lubricated bearings, Wang and Tsai [24] applied parallel computing in a thermohydrodynamic lubrication analysis. The portable parallel programming language OpenMP is applied. The result shows that the 3-D time-dependent energy equation can be solved in parallel with a high parallel efficiency of 94%. In that study, the SOR method using natural ordering conducted in parallel for the generalized Reynolds equation is poorly performed (56.5% parallel efficiency) due to the data race problem. The data race in multithread computing is the case when an iteration may occasionally use an older value from a preceding or succeeding column, rather than the latest value. Therefore, two or more statements can read or write to the same memory location at the same time causing data race. However, the iterative algorithm, such as the SOR method applied by Wang and Tsai [24], is tolerant of such errors and will still converge, but slowly, to the desired solution. Some other applications of OpenMP programming in recent tribological optimization studies can be found in Refs. [25,26].

The solution time of air foil bearing analysis can be significantly minimized by using parallel computing. The OpenMP paradigm is the de facto standard for multithread computing in today's multicore shared-memory computers. The incremental parallelization and parallel-directive format of OpenMP programming make the multithread parallel computing straightforward [27,28]. A thread in a computing is a small but independent job which can be executed in a processor core. The use of OpenMP is especially effective in multicore environments where many threads can be handled simultaneously. To have multiple threads to be executed concurrently for the discretized Reynolds equation, a parallel computing scheme is required which is to be introduced in the next section.

In this study, the problem is to solve the pressure distribution and the film profile of an air foil bearing under a given load. The thermal effects on the foil bearing properties are neglected. The solution procedure for the analysis requires a multiple-level-deep nested iteration. The main focus of this study is to generalize an efficient solution procedure for compliant surface bearing analysis using parallel iterative methods. Initially, the compressible-fluid Reynolds equation is linearized by Newton's method. The equation is then discretized and solved by one of the two parallel SOR methods using OpenMP programming. Then, a numerical damping procedure is introduced in the iterative process for pressure updating to determine the compliant foil profile for a given eccentricity. Finally, a nonlinear root-finding process is conducted to attain the eccentricity for a given load. In this study, each iteration-loop is separately dealt with for convergence and computational efficiency. The approaches adopted are also useful for other similar applications, such as air foil bearings with nonisothermal consideration, various foil materials, or different elastic foil models.

2. METHODOLOGY

2.1 The Air Foil Bearing Model

In this study, the bearing (Fig. 1) is lubricated by air and the bearing has a flexible foil surface which is supported by the bump foil (Fig. 2). The parameters of the air foil bearing are listed in Table 1 [13,29]. The air is treated as Newtonian fluid and the variation of viscosity and density across the air film direction is neglected. The condition of no-slip at the bearing surface interface is also assumed. Thus, the Reynolds equation for modeling air foil bearing lubrication can be expressed as

https://doi.org/10.1017/jmech.2012.50 Published online by Cambridge University Press

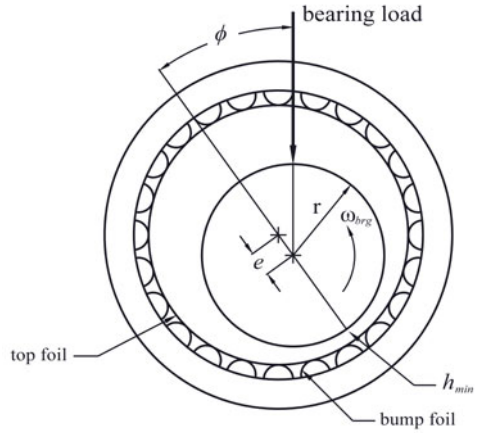


Fig. 1 The schematic of the air foil bearing of bump type

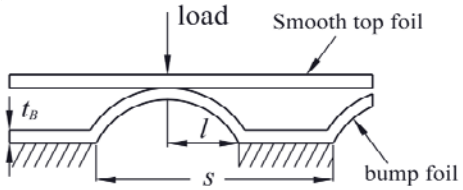


Fig. 2 A blowup view of the bump foil in Fig. 1

Table 1 The parameters of the air foil bearing [13,29]

Bearing radius, r	19.05mm
Bearing length, B	38.1mm
Bearing radial clearance, c	57μm
Bump foil thickness, t_B	101.6μm
Bump pitch, s	4.572mm
Half bump length, l	1.778mm
Bump foil Young's modulus, E	214GPa
Bump foil Poisson's ratio, ν	0.29

$$\frac{\partial}{\partial x}\left(\frac{\rho h^3}{12\mu}\frac{\partial p}{\partial x}\right)+\frac{\partial}{\partial y}\left(\frac{\rho h^3}{12\mu}\frac{\partial p}{\partial y}\right)=\frac{U}{2}\frac{\partial(\rho h)}{\partial x}.$$

In addition, the temperature of air is assumed invariant in operation and the air is treated as an ideal gas. As a result, the air is isoviscous and the density of air is proportional to the fluid film pressure, *i.e.* $\rho = p/(RT)$. Therefore, the Reynolds equation for the air foil bearing lubrication is

$$\frac{\partial}{\partial x}\left(ph^3\frac{\partial p}{\partial x}\right)+\frac{\partial}{\partial y}\left(ph^3\frac{\partial p}{\partial y}\right)=6\mu U\frac{\partial(ph)}{\partial x}. \quad (1)$$

To add the generality of the governing equation, the parameters shown in Eq. (2) are used to nondimensionalize Eq. (1).

$$\bar{x}=\frac{x}{B},\ \bar{y}=\frac{y}{B},\ \bar{p}=\frac{p\,c^2}{\mu UB},\ \bar{h}=\frac{h}{c}. \quad (2)$$

Substituting Eq. (2) into Eq. (1), which gives the following nondimensional form:

$$\frac{\partial}{\partial\bar{x}}\left(\bar{p}\bar{h}^3\frac{\partial\bar{p}}{\partial\bar{x}}\right)+\frac{\partial}{\partial\bar{y}}\left(\bar{p}\bar{h}^3\frac{\partial\bar{p}}{\partial\bar{y}}\right)=6\frac{\partial(\bar{p}\bar{h})}{\partial\bar{x}}. \quad (3)$$

In this study, Newton's (or Newton-Raphson) method is applied to linearize Eq. (3). Thus, the fluid film pressure can be solved recursively (Eq. (4)) by using the following expression:

$$\bar{p}^{n+1}=\bar{p}^n+\delta^n,\quad n=0,\ 1,\ 2,... \quad (4)$$

where δ (pressure modification) is the solution of the following equation:

$$\frac{\partial}{\partial\bar{x}}\left(\bar{p}\bar{h}^3\frac{\partial\delta}{\partial\bar{x}}+\delta\bar{h}^3\frac{\partial\bar{p}}{\partial\bar{x}}\right)+\frac{\partial}{\partial\bar{y}}\left(\bar{p}\bar{h}^3\frac{\partial\delta}{\partial\bar{y}}+\delta\bar{h}^3\frac{\partial\bar{p}}{\partial\bar{y}}\right)-6\frac{\partial(\delta\bar{h})}{\partial\bar{x}}$$
$$=-\frac{\partial}{\partial\bar{x}}\left(\bar{p}\bar{h}^3\frac{\partial\bar{p}}{\partial\bar{x}}\right)-\frac{\partial}{\partial\bar{y}}\left(\bar{p}\bar{h}^3\frac{\partial\bar{p}}{\partial\bar{y}}\right)+6\frac{\partial(\bar{p}\bar{h})}{\partial\bar{x}}. \quad (5)$$

The discretized Eq. (5) [20] is to be solved by an iterative method which can be expressed as

$$\delta_{i,j}^{n+1}=\delta_{i,j}^n+\omega\,\Delta\delta_{i,j}^{n+1},\ \text{and}\ \ \Delta\delta_{i,j}^{n+1}=(\tilde{\delta}_{i,j}^{n+1}-\delta_{i,j}^n), \quad (6)$$

where $i = 1, \ldots, nx$, $j = 1, \ldots, ny$, ω is the relaxation factor, and $\tilde{\delta}_{i,j}^{n+1}$ is the solution of Eq. (5) solved by the GS method. A useful formula for computing the optimum relaxation factor (ω_{opt}) [22] as a function of grid size is as follows:

$$\omega_{opt}=\frac{2}{1+C\,\Delta\bar{x}}, \quad (7)$$

where $\Delta\bar{x}$ is the dimensionless grid size, and C is a constant for a given problem.

In this study, the performance tests are illustrated with three sizes of gridwork (160 × 50, 320 × 100, and 480 × 150). Note that the bearing length in the x-direction is 3.14 times of the bearing width in the y-direction. The size of the numerical grids required for a converged solution is affected by the bearing geometry, eccentricity ratio, and rotating speed. It is noted that the use of the optimum relaxation factor gives a very significant improvement in the rate of convergence and it is better to overestimate than to understate the relaxation factor in an SOR method [21,22].

In this study, the stopping criteria used for Eqs. (4) and (6) are

$$\left(\Delta\bar{x}\,\Delta\bar{y}\sum_{i=0}^{nx}\sum_{j=0}^{ny}(\bar{p}_{i,j}^{n+1}-\bar{p}_{i,j}^n)^2\right)^{\frac{1}{2}}<10^{-4} \quad (8)$$

$$\left(\Delta\bar{x}\,\Delta\bar{y}\sum_{i=0}^{nx}\sum_{j=0}^{ny}(\Delta\delta_{i,j})^2\right)^{\frac{1}{2}}<10^{-5}, \quad (9)$$

respectively.

To determine the foil deformation in a bearing with a known eccentricity ratio, the air film thickness is defined by the following elastic foil model [12]:

https://doi.org/10.1017/jmech.2012.50 Published online by Cambridge University Press

$$\bar{h}^{n+1} = 1 + \varepsilon\cos\theta + \alpha(\tilde{p}^n - 1),\ n = 0,\ 1,\ 2, \ldots \quad (10)$$

where ε is eccentricity ratio, $\tilde{p}^n = p^n / p_a$, and $\alpha = \frac{2p_a s}{cE}\left(\frac{l}{t_B}\right)(1-\nu^2)$.

At the beginning of a simulation, $\bar{h}^1 = 1 + \varepsilon\cos\theta + \alpha(\tilde{p}^0 - 1)$ where $\tilde{p}^0$ is an initial guess. The value of the $\tilde{p}^0$ should prevent the minimum film thickness becoming zero or negative when the eccentricity ratio is greater or equal to unity. Next, $\bar{h}^1$ is used in Eq. (5), which can be solved to provide next pressure field by using Eq. (4). Then, a new iteration begins. The iteration is terminated when Eq. (11) is satisfied and the bearing load can then be calculated by Eq. (12),

$$\left|\frac{W(\tilde{p}^{n+1}) - W(\tilde{p}^n)}{W(\tilde{p}^{n+1})}\right| < 10^{-5}, \quad (11)$$

$$W = \iint p\, dx\, dy. \quad (12)$$

2.2 Numerical Damping

It is noticed that if $\bar{p}$, instead of $\tilde{p}$, is used in Eq. (10) the solution of the film profile may oscillate (so as the film pressure). The result is an extended iteration requirement before both the pressure and profile of the film are converged. In this study, a numerical damping procedure is introduced to minimize the solution (film profile) oscillation in Eq. (10). The function of the numerical damping is to updating the $\tilde{p}$ in a slower but stable fashion. The treatment is similar to the process of an under-relaxation method for a system of equations with a high condition number. In this study, the fluctuation of the $\tilde{p}$ is damped in the solution-seeking process (for a given ε) by using the following equation:

$$\tilde{p}^{n+1} = \frac{\mu U B}{c^2 p_a}\left(\beta(\bar{p}^{n+1} - \bar{p}^n) + \bar{p}^n\right),\ n = 0,\ 1,\ 2, \ldots \quad (13)$$

where $\tilde{p}$ is the film pressure normalized to p_a, and β is the numerical damping constant ($0 < \beta \le 1$).

A proper β makes the solution converged faster and allows the use of a large relaxation factor. If $\beta = 1$, no damping effect is achieved.

2.3 The Root-Finding Procedure

In the case of a given bearing load, the solution of the final film profile of the bearing and the corresponding film pressure can be obtained in many ways. Note that the compliant foil profile is a function of eccentricity ratio (Eq. (10)). The resultant film profile which can produce a load equals the applied load has a corresponding eccentricity ratio. This can be solved as a nonlinear root-finding problem. The secant method for root-find problem is known for its efficiency but comes with a high possibility of solution divergence. The approach, thus, is to apply a hybrid procedure which starts from a slow but stable piece-wise search. The purpose of the piece-wise search is to bracket the root (ε) in a narrow range. The root-finding process can then switch to the secant method. The iteration is terminated when the following convergence criterion is met.

$$\left|\frac{\varepsilon^{n+1} - \varepsilon^n}{\varepsilon^{n+1}}\right| < 10^{-4}. \quad (14)$$

2.4 Parallel SOR Methods

In this study, two parallel SOR methods of domain decomposition are tested as the solution solver for Eq. (5). The parallel programming paradigm is OpenMP. The concept of domain decomposition is to divide the computational work into several tasks which can be executed in parallel. The domain decomposition can be carried out in a number of ways. In this study, two popular and easy to implement methods, strip partition SOR (SPSOR) and red-black SOR (RBSOR) methods, are applied to solve Eq. (5). Figure 3 illustrates the layout of the SPSOR method. In the SPSOR iteration, the interior points of each strip are treated as in a regular SOR method. The number of the strips divided in the numerical gridwork is equal to the number of available processor cores. As a result, each processor core can execute one thread. And all the threads can be processed at the same time. The direction of the strip dividing is determined by minimizing the divided boundary points, which is parallel to the y-axis in this study.

It is noted that the points in the right-most column of strip 1 in Fig. 3 requires the value of the left-most points in the strip 2. The similar situation appears in the other strips. Since the computation in each strip is conducted concurrently, the updating process for the points along the strip boundaries might not have the updated data (the so-called data race problem). Nevertheless, in this iterative procedure the data race degrades the performance but not preventing the convergence. It is expected that the more strips in a parallel computing the more severe the data race problem is. The result is an increase of number of iterations for the same convergence criterion.

The RBSOR method adopts a different strategy in preparing the parallel computing. The domain of the computation is divided in to a two-partition layout (Fig. 4), and each partition is denoted by red (circle) or black (triangular) points. If the computation starts from the red points, then this five-point finite difference stencil computation of the discretized Eq. (5) depends on the values of the adjacent four black points. Other than the boundary points the values of the black points are from a previous iteration or initial guess. The computation of all red points can be executed in parallel among the available processor cores. The next step to complete the whole domain computation is to perform the black-point calculation. Similar operation as the

https://doi.org/10.1017/jmech.2012.50 Published online by Cambridge University Press

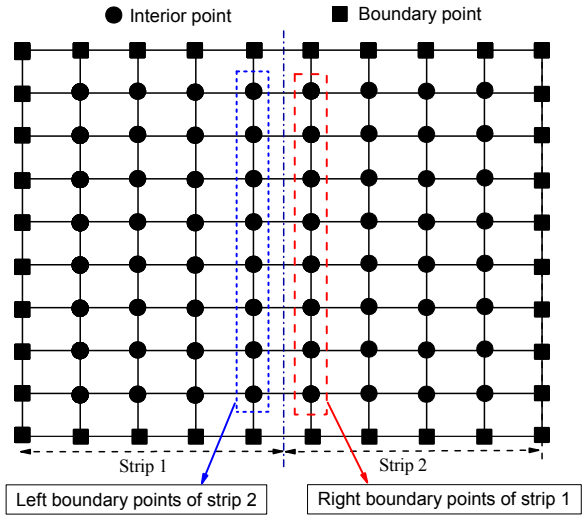


Fig. 3 The layout of a two-strip SPSOR method. The five-point finite difference stencil computation is used

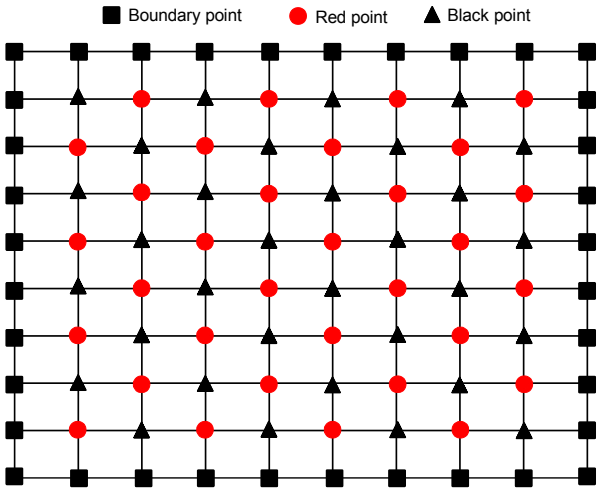


Fig. 4 The layout of the RBSOR method. The five-point finite difference stencil computation is used

red-point is carried out, but the updating is with the newly computed red points which can accelerate the convergence. No data race problem is encountered in the RBSOR method.

The ω_{opt} used in the SPSOR and RBSOR methods for gridwork of 160 × 50 are 1.80, and 1.83, respectively. These numbers are obtained by numerical tests. Thus, the values of ω_{opt} for the gridwork of 320x100 and 480 × 150 can be computed by using Eq. (7). The results are listed in Table 2.

2.5 The Computational Platform and Flowchart

The workstation used in this study is a HP Z600 workstation. It has two quad-core Intel Xeon/2.0GHz CPUs and 8GB main memory. Therefore, the system has eight processor cores, which can process eight threads simultaneously using OpenMP programming. The operation system is Microsoft Windows 7. The programming language is Fortran 90 and the compiler

Table 2 The optimum relaxation factors (ω_{opt}) used in SPSOR and RBSOR methods

Gridwork	SPSOR Method	RBSOR Method
160 × 50	1.800	1.830
320 × 100	1.895	1.911
480 × 150	1.929	1.940

is Intel Visual Fortran Ver. 11. For a today's complex operating system the execution time of the program is affected more or less by some background activities. Instead of averaging the execution time, the execution time in this parallel computing study is obtained by running the same case five times and record the one with shortest elapsed time. This should better reflect the actual time used in computing.

Figure 5 shows the multiple-level-deep nested iteration procedure for the analysis of air foil bearings. The inner-most-loop is the solution loop for δ (Eq. (6)) by one of the parallel SOR methods. The second-loop is the outer iteration loop of Newton's method (Eq. (4)) in order to solve Eq. (5). The third-loop is for the film pressure of a given ε. And the outer-most-loop is for finding the film profile (ε) to match the given bearing load. It can be seen that the number of calculations required for solving Eq. (5) can be enormous in an air foil bearing analysis. The execution time, thus, is proportional to the solution time of Eq. (5). And the reduction of iteration in each level can also lower the overall computational effort.

3. RESULTS AND DISCUSSION

In this study, the developed computer model is verified by examining the numerical results, the minimum film thickness versus the bearing load, with the published experimental data [29]. The case examined is shown in Fig. 6. A similar comparison is also conducted by San Andres and Kim [13] with good agreement. It can be seen that the simulation results conform the experimental data in both the magnitude and the trend. Note that the initial minimum film thickness (null bearing load) should equal the radial clearance of the bearing.

The solution oscillation shown in Fig. 7 illustrates the process in seeking the balanced air film pressure and the compliant foil profile (Eq. (13)) for a given shaft position (ε). In this case, no numerical damping is used in updating the air film pressure. It can be seen that the solution is converged but in a very slow rate. At least 200 iterations are required before the solution converged. If a numerical damping (β = 0.2, 0.4, 0.6, or 0.8, and ε = 0.8 in this case) is applied in the pressure updating process (Eq. (13)) the solution oscillation is reduced or eliminated (Fig. 8). More importantly, the number of iterations required is significantly reduced by using the numerical damping. To avoid the oscillation of the solution in a possible high eccentricity ratio case (the final ε = 1.61), β = 0.2 is used in

https://doi.org/10.1017/jmech.2012.50 Published online by Cambridge University Press

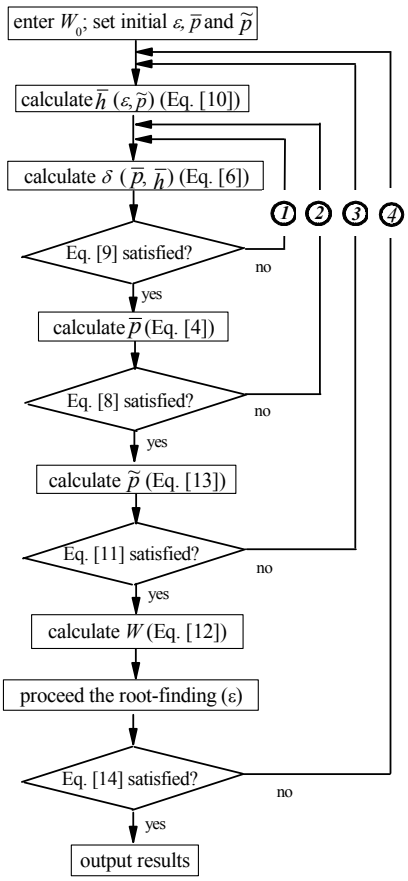


Fig. 5 The multiple-level-deep nested iteration of the air foil bearing analysis. The numbers in circle denote the iteration level. The loop number 1 is the inner-most iteration

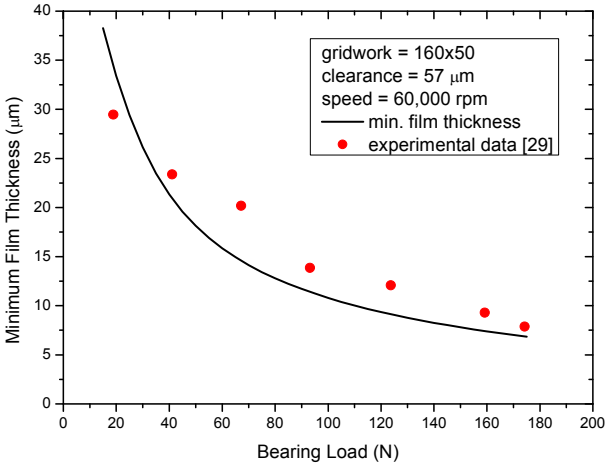


Fig. 6 Comparison of the minimum film thickness along the mid-plane of the bearing under various loading of the developed computer model and the experimental data [29]

the performance study. Note that the eccentricity ratio in Eq. (10) can be greater than one. It is found that a small numerical damping can have a more effective result when the bearing load or the eccentricity ratio is large.

The stability performance of a high speed (circular) journal bearing is usually judged by the attitude angle.

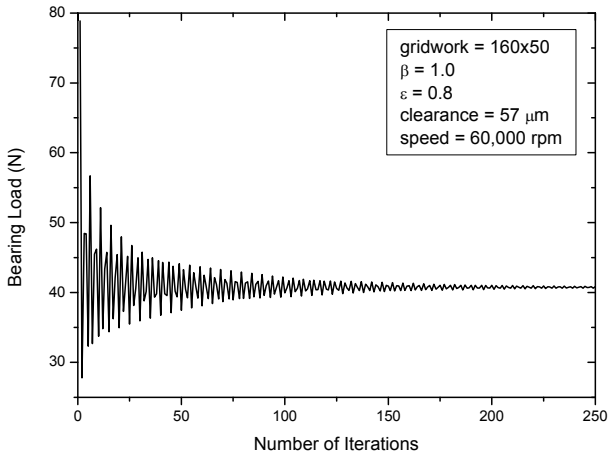


Fig. 7 The oscillation of bearing load in updating the air film pressure. The oscillation is due to the undamped (β = 1) pressure updating by Eq. (13)

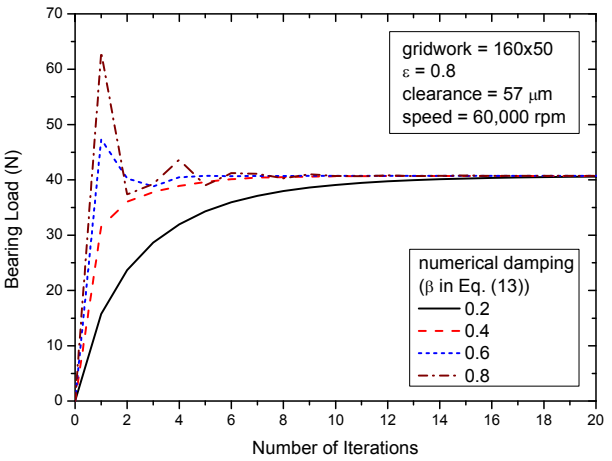


Fig. 8 The effect of the numerical damping on the convergence of the solution of bearing load

The smaller the attitude angle typically means the more stable the bearing is to operate in high speed. One of the advantages of air foil bearings is having a small attitude angle at high speed. Figure 9 shows the performance prediction obtained in this study. The bearing load capacity is increased as the bearing speed is increased, which is expected due to the dynamic effect of the lubricant.

The study of computation efficiency in using the parallel SOR (*i.e.*, SPSOR and RBSOR) methods is presented by using the case of W_s = 150N, speed = 60,000rpm, and c = 57μm. The SPSOR or RBSOR method is used to parallelize the computational work of discretized Eq. (5). The parallel programming is conducted by using OpenMP directives. The other parts of the solution procedure are the same for the two approaches. The numerical gridwork used is 160 × 50, and the optimum relaxation factors for the SPSOR and RBSOR methods are 1.80 and 1.83, respectively. The resultant film pressure and thickness of the bearing are shown in Fig. 10. The minimum film thickness is 7.79 μm, the eccentricity ratio is 1.61, and the attitude angle is 11.96°.

https://doi.org/10.1017/jmech.2012.50 Published online by Cambridge University Press

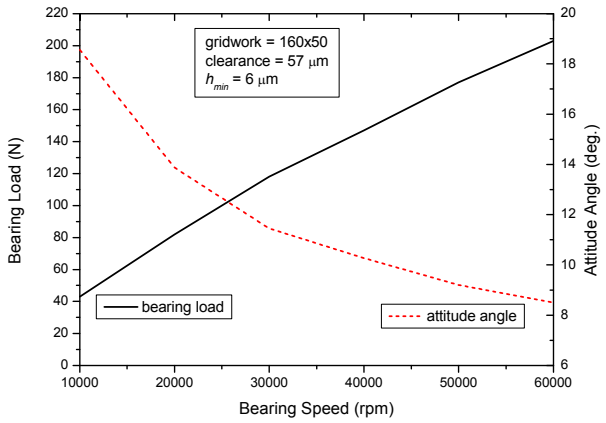


Fig. 9 The bearing performance (load capacity and attitude angle) as the function of bearing speed

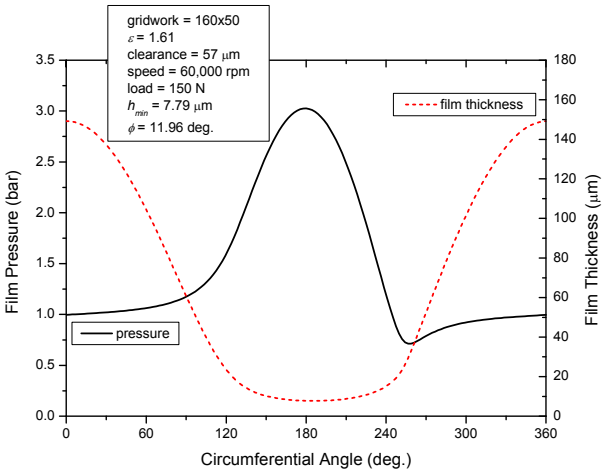


Fig. 10 The mid-plane (in the direction of sliding) air film pressure and the film thickness of the air foil bearing

The speedups of the SPSOR and RBSOR methods using various processor cores (1, 2, 4, and 8) are plotted in Fig. 11. The speedup is the performance measurement for an application executed in single thread relative to multiple threads. The ideal (maximum) speedup of a machine is equal to the number of available processor cores. In Fig. 11, the numbers of iterations in the SPSOR and RBSOR methods with eight processor cores are 23,195 (2.163s) and 24,096 (1.991s), respectively. The relatively low speedups (3.76 and 3.85) of the eight-thread cases are due to the high frequency of communication requirement (in each iteration) in parallel computing. The average execution times including the computational and communication times in one iteration for SPSOR and RBSOR methods are 93.3 and 82.6μs, respectively.

The results of the performance test for finer grids by the SPSOR and RBSOR methods are shown in Figs. 12 and 13, respectively. As expected, the speedup for both methods is higher as the grid size becomes finer. This is due to a longer solution time is required in a finer grid case and the percentage of communication overhead relative to the overall execution time is decreased. It can be seen that the RBSOR method demonstrates a faster execution and a higher speedup than the SPSOR

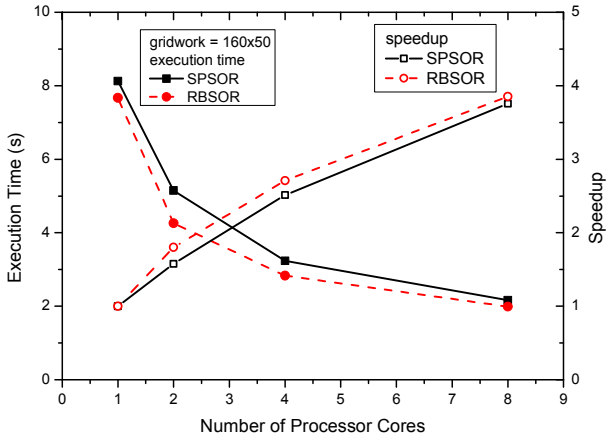


Fig. 11 The performance of the parallel SOR methods for the gridwork of 160 × 50

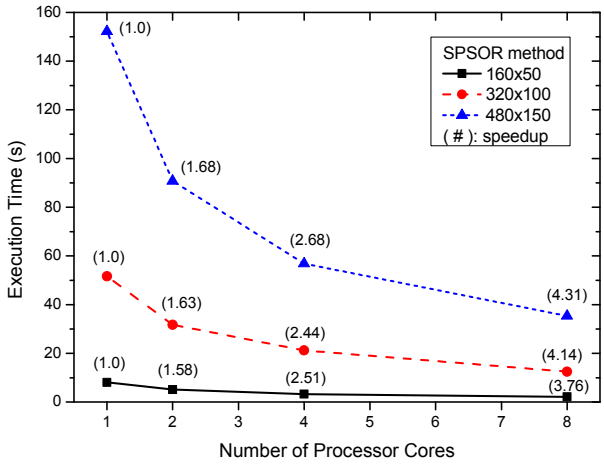


Fig. 12 The performance of the parallel SPSOR method for different sizes of gridwork

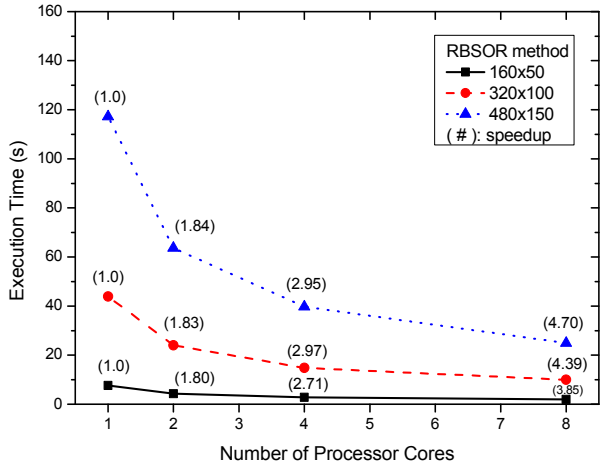


Fig. 13 The performance of the parallel RBSOR method for different sizes of gridwork

method. The lower rate of convergence of SPSOR method may be due to the data race problem along the divided strip boundaries. The computational sequence of the RBSOR method is also more efficient, which can be judged by the performance of the two methods when one processor core is used.

Table 3 lists the number of iterations required for the optimum SOR and GS methods by using one processor

https://doi.org/10.1017/jmech.2012.50 Published online by Cambridge University Press

Table 3 The numbers of iteration in using sequential RBSOR and SPSOR methods with unity and optimal relaxation factors

Gridwork	SPSOR Method		RBSOR Method	
	$\omega = 1.0$	ω_{opt}	$\omega = 1.0$	ω_{opt}
160 × 50	68,210	23,170	75,966	24,096
320 × 100	619,513	35,116	795,073	34,215
480 × 150	N/C	44,761	N/C	40,785

N/C: not converged; ω_{opt}: see Table 2

core. It can be seen that the number of iterations in the cases by the GS method can be much larger than those by the optimum SOR methods. For the case of gridwork 480 × 150 the solution of the GS method is not converged. Note that the number of iterations in the SPSOR method for the cases of more than one processor core is slightly increased due to the minor data race problem. While the number of iterations required in the RBSOR method is independent of the number of processor cores used.

4. CONCLUSIONS

It is demonstrated that the solution procedure in the analysis of isothermal air foil bearings requires a multiple-level-deep nested iteration to solve the problem. In this study, several methods are tailored to provide a fast solution scheme for air foil bearing analyses. These methods include the parallel SOR methods, the procedure to damp the oscillation solution in the pressure updating process, and the method to solve the root-finding problem effectively. The importance of using optimum relaxation factor and numerical damping (especially in the cases with large bearing numbers and high eccentricity ratios) is emphasized. It is also noted that today's workstations, within the financial reach of most researchers, are capable of handling very small (fine-grain) tasks efficiently using multiple processor cores and OpenMP programming.

Some studies [16,17] for air foil bearing analysis reported that extended solution time is required in the cases with large bearing numbers and high eccentricity ratios. Nevertheless, the SUR method is used in these studies and an extended solution time is resulted. In the proposed solution procedure (Fig. 5) the much fast optimum SOR method is used in solving Reynolds equation, and the introduction of numerical damping process ensure a fast rate of convergence in the nonlinear root-finding problem. For a large bearing load, however, a small numerical damping is required.

The execution time of other complex air foil bearing problems can be increased significantly when additional conditions are superimposed on top of the basic model presented in this study. These may involve the thermal consideration for air viscosity or material property changes, and the optimum design of air foil bearings. In these cases, the solution of energy equation and an efficient global search scheme are required. Nevertheless, the basic model of the air foil bearing (*e.g.*, an air foil bearing with given geometry and running conditions) is to be solved frequently. Using the solution scheme outlined in this study the solution time for the basic model can be minimized. The applications of that basic model can then be solved effectively.

The power law scheme provides a fast and stable solution for some foil bearing analyses [7]. The fast solution of power law scheme is due to it can apply coarse grid computation with power law interpolation. However, the solution of power law scheme will approach first-order accurate for high bearing numbers and may be inaccurate for the flow oblique or skew to the grids [30]. The classical second-order finite difference method presented and solved by parallel SOR methods can handle discontinued boundary conditions such as in externally pressurized air bearings. The instability encountered in high bearing numbers can be solved by using the numerical damping presented in this study.

Computers of nowadays are equipped with multicore CPUs. Some workstations have more than one such multicore CPUs installed. Most of the compilers for C, C^{++} and Fortran languages are also OpenMP-supported. It is very hard to justify not using a few OpenMP directives to parallel the bottleneck of the program. Surprisingly, the poorly performed GS method is still being used for no good reason in some tribological studies [16,17,19]. In this study, the optimum SOR methods make the solution convergence possible for the cases using fine-grids. The high speedups obtained in parallel computing are also resulted for the same reason. It is recommended that the solution scheme for the analysis of air foil bearings is to follow the procedure outlined in Fig. 5, and use the RBSOR method as the parallel computing tool to minimize the number of iterations and solution time.

ACKNOWLEDGMENTS

This study is supported by the National Science Council of ROC, Contract number NSC99-2221-E-182-014.

NOMENCLATURES

B = width of bearing
c = radial clearance of bearing
C = constant used in Eq. (7)
e = eccentricity of bearing
E = Young's modulus of bump foil
h = fluid film thickness
$h_{\min}$ = minimum fluid film thickness
$\bar{h}$ = dimensionless fluid film thickness
l = length of half bump foil
nx, ny = number of gridworks in x- and y-direction
p = fluid film pressure
$\bar{p}$ = dimensionless fluid film pressure

$$\left(\bar{p} = \frac{p\, c^2}{\mu\, UB} \right)$$

https://doi.org/10.1017/jmech.2012.50 Published online by Cambridge University Press

$\tilde{p}$ = dimensionless fluid film pressure $\left(\tilde{p} = \frac{p}{p_a}\right)$

p_a = atmospheric pressure
r = radius of bearing shaft
s = pitch of bump foil
t_B = bump foil thickness
U = bearing velocity
W = bearing load capacity
$\bar{x}$, $\bar{y}$ = dimensionless coordinates
α = bump foil compliance number (Eq. (10))
β = numerical damping constant (Eq. (13))
δ = modification of $\bar{p}$ (Eq. (4))
$\tilde{\delta}$ = solution of δ obtained by Gauss-Seidel method (Eq. (6))
ε = eccentricity ratio of bearing
θ = circumferential angle of journal bearing
μ = lubricant viscosity
ν = Poisson's ratio of bump foil
ϕ = attitude angle
ω = relaxation factor
ω_{brg} = rotating speed of bearing
ω_{opt} = optimum relaxation factor
$\Delta\bar{x}$, $\Delta\bar{y}$ = dimensionless grid size in x- and y-direction
$\Delta\delta$ = residual of δ

Subscripts and Superscript

i, j = indices for grid in x- and y-direction
n = index of iteration

REFERENCES

1. DellaCorte, C., Radil, K. C., Bruckner, R. J. and Howard, S. A., "Design, Fabrication, and Performance of Open Source Generation I and II Compliant Hydrodynamic Gas Foil Bearings," *Tribology Transactions*, **51**, pp. 254–264 (2008).
2. Jahanmir S., Heshmat, H. and Heshmat, C., "Assessment of Tribological Coatings for Foil Bearing Applications," *Tribology Transactions*, **52**, pp. 231–242 (2009).
3. Jahanmir, S., Heshmat, H. and Heshmat, C., "Evaluation of DLC Coatings for High-Temperature Foil Bearing Applications," *Journal of Tribology – Transactions of the ASME*, **131**, pp. 011301.1–011301.11 (2009).
4. Feng, K. and Kaneko, S., "Thermohydrodynamic Study of Multiwound Foil Bearing Using Lobatto Point Quadrature," *Journal of Tribology – Transactions of the ASME*, **131**, pp. 0212702.1–0212702.9 (2009).
5. Lee, D. and Kim, D., "Thermohydrodynamic Analyses of Bump Air Foil Bearings With Detailed Thermal Model of Foil Structures and Rotor," *Journal of Tribology – Transactions of the ASME*, **132**, pp. 0212704.1–0212704.12 (2010).
6. Lee, D. and Kim, D., "Three-Dimensional Thermohydrodynamic Analyses of Rayleigh Step Air Foil Thrust Bearing with Radially Arranged Bump Foils," *Tribology Transactions*, **54**, pp. 432–448 (2011).
7. Song, J. H. and Kim, D., "Foil Gas Bearing with Compression Springs: Analyses and Experiments," *Journal of Tribology – Transactions of the ASME*, **129**, pp. 628–639 (2007).
8. Kim, T. H. and San Andres, L., "Thermohydrodynamic Model Predictions and Performance Measurements of Bump-Type Foil Bearing for Oil-Free Turboshaft Engines in Rotorcraft Propulsion Systems," *Journal of Tribology – Transactions of the ASME*, **132**, pp. 011701.1–011701.11 (2010).
9. Lee, D., Kim, D. and Sadashiva, R. P., "Transient Thermal Behavior of Preloaded Three-Pad Foil Bearings: Modeling and Experiments," *Journal of Tribology – Transactions of the ASME*, **133**, pp. 021703.1–021703.11 (2011).
10. Howard, S. A., DellaCorte, C., Valco, M. J., Prahl, J. M. and Heshmat, H., "Dynamic Stiffness and Damping Characteristics of a High Temperature Air Foil Journal Bearing," *Tribology Transactions*, **44**, pp. 657–667 (2001).
11. Radil, K., DellaCorte, C. and Zeszotek, M., "Thermal Management Techniques for Oil-Free Turbomachinery Systems," *Tribology Transactions*, **50**, pp. 319–327 (2007).
12. Heshmat, H., Walowit, J. A. and Pinkus, O., "Analysis of Gas-Lubricated Foil Journal Bearings," *Journal of Lubrication and Technology*, **105**, pp. 647–655 (1983).
13. San Andres, L. and Kim, T. H., "Analysis of Gas Foil Bearings Integrating FE Top Foil Models," *Tribology International*, **42**, pp. 111–120 (2009).
14. Salehi, M. and Heshmat, H., "On the Fluid Flow and Thermal Analysis of a Compliant Surface Foil Bearing and Seal," *Tribology Transactions*, **43**, pp. 318–324 (2000).
15. Lee, N. S., Choi, D. H., Lee, Y. B., Kim, T. H. and Kim, C. H., "The Influence of the Slip Flow on Steady-State Load Capacity, Stiffness and Damping Coefficients of Elastically Supported Gas Foil Bearings," *Tribology Transactions*, **45**, pp. 478–484 (2002).
16. Peng, Z.-C. and Khonsari, M. M., "Hydrodynamic Analysis of Compliant Foil Bearings with Compressible Air Flow," *Journal of Tribology – Transactions of the ASME*, **126**, pp. 542–546 (2004).
17. Peng, Z.-C. and Khonsari, M. M., "A Thermohydrodynamic Analysis of Foil Journal Bearings," *Journal of Tribology – Transactions of the ASME*, **128**, pp. 534–541 (2006).
18. Park, D.-J., Kim, C.-H., Jang, G.-H. and Lee, Y.-B., "Theoretical Considerations of Static and Dynamic Characteristics of Air Foil Thrust Bearing with Tilt and Slip Flow," *Tribology International*, **41**, pp. 282–295 (2008).

https://doi.org/10.1017/jmech.2012.50 Published online by Cambridge University Press

19. Iordanoff, I., Bou-Said, B., Mezianne, A. and Berthier, Y., "Effect of Internal Friction in the Dynamic Behavior of Aerodynamic Foil Bearings," *Tribology International*, **41**, pp. 387–395 (2008).
20. Wang, N. and Chang, C., "An Application of Newton's Method to the Lubrication Analysis of Air-Lubricated Bearing," *Tribology Transactions*, **42**, pp. 419–424 (1999).
21. Strikwerda, J. C., *Finite Difference Schemes and Partial Differential Equations*, Pacific Grove: Wadsworth and Brooks (1989).
22. Morton, K. W. and Mayers, D. F., *Numerical Solution of Partial Differential Equations*, Cambridge: Cambridge University Press (2005).
23. Wang, N., Chang, S.-H. and Huang, H.-C., "Comparison of Iterative Methods for the Solution of Compressible-Fluid Reynolds Equation," *Journal of Tribology – Transactions of the ASME*, **133**, pp. 021702.1–021702.7 (2011).
24. Wang, N. and Tsai, C.-M., "Application of Thread-Level Parallel Programming to Thermohydrodynamic Lubrication Computation," *Tribology Transactions*, **49**, pp. 473–481 (2006).
25. Wang, N., Tsai, C.-M. and Cha, K.-C., "A Study of Parallel Efficiency of Modified DIRECT Algorithm Applied to Thermohydrodynamic Lubrication," *Journal of Mechanics*, **25**, pp. 143–150 (2009).
26. Wang, N., Tsai, C.-M. and Cha, K.-C., "Optimum Design of Externally Pressurized Air Bearing Using Cluster OpenMP," *Tribology International*, **42**, pp. 1180–1186 (2009).
27. Chapman, B., Gost, G., van der Pas, R. and Kuck, D. J., *Using OpenMP: Portable Shared Memory Parallel Programming*, Cambridge: The MIT Press (2008).
28. Chandra, R., Dagun, L., Kohr, D., Maydan, D., McDonald, J. and Menon, R., *Parallel Programming in OpenMP*, San Francisco: Academic Press (2001).
29. Ruscitto, D., Mc Cormick, J. and Gray, S., "Hydrodynamic Air Lubricated Compliant Surface Bearing for an Automotive Gas Turbine Engine I - Journal Bearing Performance," NASA CR-135368 (1978).
30. Leonard, B. P. and Drummond, J. E., "Why You Should Not Use Hybrid, Power-Law or Related Exponential Schemes for Convective Modeling—There Are Much Better Alternatives," *International Journal for Numerical Methods in Fluids*, **20**, pp. 421–442 (1995).

(Manuscript received June 10, 2011,
accepted for publication November 10, 2011.)

https://doi.org/10.1017/jmech.2012.50 Published online by Cambridge University Press